Closed-loop structural control with real-time smart sensors

Lauren E. Linderman[*1] and Billie F. Spencer Jr.[2a]

[1]*Department of Civil, Environmental, and Geo- Engineering, University of Minnesota,*
500 Pillsbury Drive S.E., Minneapolis, MN 55455, USA
[2]*Department of Civil and Environmental Engineering, University of Illinois,*
205 N. Mathews Ave., Urbana, IL 61801, USA

Abstract. Wireless smart sensors, which have become popular for monitoring applications, are an attractive option for implementing structural control systems, due to their onboard sensing, processing, and communication capabilities. However, wireless smart sensors pose inherent challenges for control, including delays from communication, acquisition hardware, and processing time. Previous research in wireless control, which focused on semi-active systems, has found that sampling rate along with time delays can significantly impact control performance. However, because semi-active systems are guaranteed stable, these issues are typically neglected in the control design. This work achieves active control with smart sensors in an experimental setting. Because active systems are not inherently stable, all the elements of the control loop must be addressed, including data acquisition hardware, processing performance, and control design at slow sampling rates. The sensing hardware is shown to have a significant impact on the control design and performance. Ultimately, the smart sensor active control system achieves comparable performance to the traditional tethered system.

Keywords: smart sensors; structural control; discrete-time control design

1. Introduction

Structural control systems offer an alternative to traditional design to limit structural response to extreme loading, including earthquake and wind. In feedback control systems, a supplemental device is used in conjunction with measurement feedback to offer improved performance over a larger frequency bandwidth and variety of loading (Housner *et al*. 1997). Independent of the supplemental device used, the closed-loop digital control system consists of sensors, i.e., displacement or acceleration, sensor processing, control calculation, and control application. Early research in the field of structural control addressed challenges in the digital control loop, including quantization, time delay, and model size, to successfully implement and improve performance of control strategies (Soong 1990, Sain *et al*. 1992, Chu *et al*. 1995, Dyke *et al*. 1996). However, as computer and sensor performance has improved, the initial challenges of implementing digital, structural control have become avoidable.

∗Corresponding author, Assistant Professor, E-mail: llinderm@umn.edu
[a] Newmark Endowed Chair in Civil Engineering., E-mail: bfs@illinois.edu

Recently, wireless smart sensors have become an exciting approach for monitoring of civil infrastructure. As smart sensors become cheaper and research in the area continues, dense deployments have been encouraged (Jo *et al.* 2011). These wireless smart sensors include onboard processing, memory, communication, and sensor interfaces. Their onboard capabilities in combination with an actuation interface make wireless sensor networks (WSN) an attractive alternative to tethered systems for control applications as well (Lynch and Loh 2006). However, wireless smart sensors pose inherent challenges for control, including communication delays, processing time, and unreliable communication. Thus, the use of WSN for structural control requires reexamination of challenges in the digital control loop, particularly sample rate, system model for design, and delay compensation.

One key challenge for wireless control is the sampling rate performance of the system. Several components of the wireless control loop impact the overall sampling rate: wireless communication, data acquisition, and processing time. For centralized wireless sensor data feedback, a time-division-multiple-access approach (TDMA) is often used to improve communication reliability and offer consistent performance (Linderman *et al.* 2013). Consequently, as the number of nodes in the network increases, the overall sampling rate goes down. Independent of wireless feedback, the type of analog to digital converter (ADC) and processing performance can have a significant impact on sampling rate performance. A pipeline style ADC can introduce as much as 30 milliseconds of latency in data acquisition (Linderman *et al.* 2015). Lynch *et al.* (2008) present the resulting wireless control sampling rate on a three-story structure fitted with MR dampers when communication and processing are considered. The sampling rate for the wireless system, 12.5 Hz, is significantly lower than the tethered system, 200 Hz.

As illustrated by Lynch *et al.* (2008), a slow sampling rate can negatively impact the performance of your control system. An absolute minimum for control is to sample at a rate at least twice the system bandwidth to avoid aliasing of the higher dynamics (Franklin *et al.* 1998). However, to approximate a discrete control system as continuous, the sample rate should be about thirty to fifty times the highest mode of interest (Hirata and Powell 1990; Franklin *et al.* 1998). Otherwise, the discrete sample time should be considered in the modeling, because lower sampling rates can lead to poor disturbance rejection and may result in a large time delay between the measurement and control application (Hirata and Powell 1990). For active control systems, the results of slow sampling rates and delays can be more severe, causing the control system to go unstable (Chu *et al.* 2002).

Research in wireless control has focused on semi-active systems, which are guaranteed to be stable, so the sampling performance does not need to be directly accounted for in the design. However, the impact of the sampling rate is evident in the performance of the controllers. Despite more system knowledge, the experimental wireless systems with communication do not perform as well as wired due to the low sampling rates (Wang *et al.* 2006, Lynch *et al.* 2008). A decentralized control system, which requires little to no communication feedback, often offers comparable performance to the wired system because of the higher sampling rate (Wang et al. 2006, Wang *et al.* 2007). In general, consideration of the sampling rate and time delay in the design also offers an improvement in performance (Loh *et al.* 2007, Wang *et al.* 2007). Therefore, even for stable systems, sampling rate is not the sole consideration, but time delays and acquisition should be considered in the design as well.

To date, the only reported use of wireless sensors for active structural control has been by Casciati and Chen (2012), who examined centralized control of a three-story, steel structure fitted with an active mass driver (AMD). The wireless system is able to achieve comparable

performance to the wired system when the building is subjected to a sinusoidal excitation due to a frequency division multiplexing (FDM) technique. The performance of the system is promising; however, the time required for the wireless sensing protocol used alongside the FDM technique and the resulting impact on the overall controller sample rate is not addressed. The sampling rate performance could be significant, if the system were to be scaled, because the number of communication channels and wireless transceivers required at the controller node will increase linearly as the number of remote sensors increases.

This work addresses control design at slow sampling rates and the impact of smart sensor hardware on control to ultimately achieve active control with smart sensors. Because active control systems do not guarantee stability, their application requires attention to all elements of the control system, including control design at slow sampling rates, data acquisition hardware, and processing performance, which are typically neglected. A single-story experimental setup fitted with an active mass driver (AMD) is controlled with a smart sensor platform. Two different acquisition approaches are considered to highlight the importance of hardware in the control loop. Ultimately, through careful control design and hardware selection, the smart sensor system achieves comparable performance to the traditional tethered system.

2. Wireless sensor platform

Of the many wireless smart sensing platforms available for control and active sensing applications (Lynch and Loh 2006, Swartz *et al.* 2005), the Imote2 was selected for this work because it is well suited for real-time, high processing applications. The Imote2, shown in Fig. 1, offers a high and variable processing speed, large onboard memory, and relatively low power consumption. The XScale PXA271 processor allows for variable processing speeds, including 13, 104, 208, and 416 MHz, that can be selected based on performance and power consumption goals. In addition, the higher processing speed allows control computations to be completed quickly to limit latency. The onboard memory consists of 32 MB of flash, 256 KB SRAM, and 32 MB of SDRAM, that allows for embedding control and estimation algorithms. The Imote2 utilizes the popular CC2420 low-power radio that can be combined with an onboard or external antenna for wireless communication over the 2.4 GHz band using the IEEE 802.15.4 protocol.
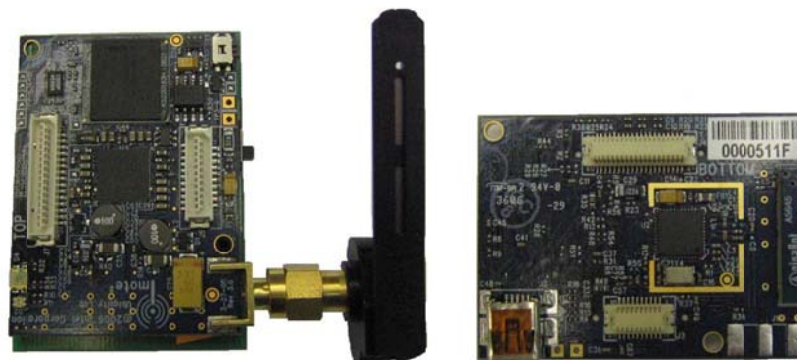

Fig. 1 Imote2 Smart Sensor Platform

2.1 Sensing interface

The Imote2 platform does not provide an onboard ADC, instead allowing it to interface with a user-selected sensor board over its basic connectors. Two sensor boards are considered in this study to compare performance for control applications. The first, designed for SHM applications, offers high-sensitivity accelerometers and high-resolution analog-to digital conversion (ADC). The second is tailored for low-latency, real-time applications.

2.1.1 SHM-A sensor board

Although designed for monitoring applications, the SHM-A was selected for this work among commercially available sensor boards due to its high-sensitivity accelerometers, high-resolution ADC, and user-selectable sensing parameters (Rice and Spencer 2009). The sensor board, shown in Fig. 2(a), includes a three-axis accelerometer (ST Microelectronics LIS344ALH), temperature and humidity sensor (Sensiron SHT11), light sensor (TAOS 2561), and an external 16-bit analog input. The four analog signals interface with a 16-bit oversampling, pipeline type ADC (QF4A512), which offers user selectable anti-aliasing filters and sampling rates.

2.1.2 SHM-SAR sensor board

The SHM-SAR, designed for low-latency applications, is considered for this work due to its ADC architecture, user selectable sampling rate, and the flexibility of the sensor interface (Linderman *et al.* 2015). The SHM-SAR, shown in Fig. 2(b), offers four analog inputs or an onboard three-axis accelerometer (ST Microelectronics LIS344ALH), which can be selected using a switch. The onboard ADC is a Successive Approximation Register (SAR) type, which completes the conversion within one sampling interval using a binary search algorithm. In comparison to pipeline-style ADCs that are more common in SHM applications, the latency due to the hardware alone is reduced from 30 milliseconds to on the order of a couple hundred microseconds (Linderman *et al.* 2015). Therefore, this ADC introduces almost no latency in the control system.

2.2 Actuation Interface

The control loop is completed with an actuation board that interfaces with the Imote2. The SHM-D2A, shown in Fig. 3, converts a command calculated on the Imote2 to an analog output voltage. The board uses a four-channel DAC (TI AD8565) that offers comparable resolution and speed to the SHM-SAR; thus, no performance is lost by the actuation interface (Linderman *et al*. 2015). Because the Imote2 offers two SPI interfaces, the actuation board can easily be combined with a data acquisition board by stacking them. Fig. 3 illustrates the SHM-D2A stacked on the SHM-SAR and Imote2 for combined sensing and actuation.

2.3 Embedded software

As with many wireless sensor platforms (Lynch and Loh 2006), the Imote2 uses the TinyOS operating system, which is tailored to the specific requirements of wireless sensor network applications. The TinyOS operating system supports an event-driven concurrency model, in which tasks are completed in a first-in-first-out (FIFO) manner along with interrupts (Levis *et al.* 2005). Thus, two main execution methods are possible: a task posted to a queue and an asynchronous interrupt.

(a) SHM-A Sensor Board   (b) SHM-SAR Sensor Board
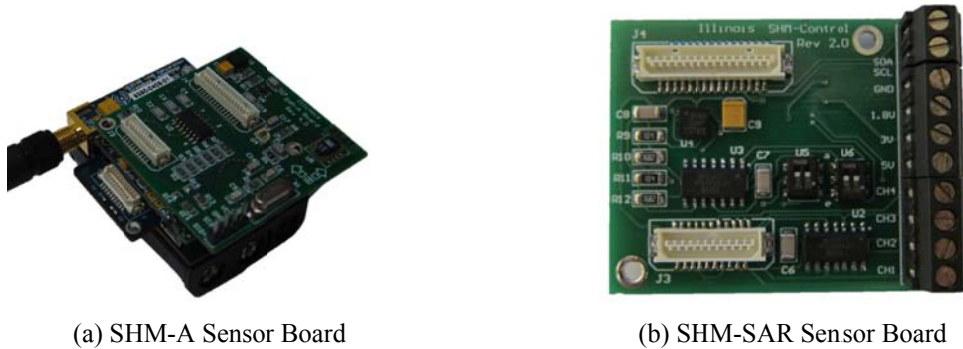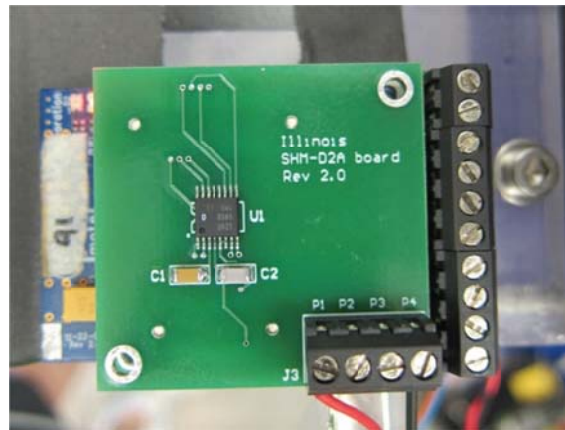
Fig. 2 Sensing Interfaces Considered with Imote2

Fig. 3 SHM-D2A for Actuation Stacked on an Imote2 and SHM-SAR

In general, the operating system (OS) is well suited for wireless applications, because the OS has a small memory footprint while being able to efficiently support complex problems. However, the FIFO nature of the system can limit the sampling rate performance for applications that require real-time feedback (Linderman *et al.* 2013). Therefore, control algorithms implemented on the sensor platform need to account for the tight timing requirements of the OS and reduce the number of tasks required.

The software used in this work is part of the open-source Illinois Structural Health Monitoring (ISHMP) Services Toolsuite (http://shm.cs.uiuc.edu/software/html). Similar to a component-based operating system, the software toolsuite uses a modular service-oriented architecture. The framework consists of three main elements: foundation services, application (domain-specific) services and tools and utilities (Rice *et al.* 2011). A typical application would combine several foundation and application services.

As an example of the embedded software, the structural control application using smart sensor nodes combines the foundation services: time synchronization and reliable communication, with real-time sensing and actuation (Fig. 4). Within the continuous sensing and commanding portion,

as shown in Fig. 5 for the SHM-A, a tightly timed approach is used to maintain consistent actuation command intervals. Alarms are set at a specified interval after the sensing event to maintain better scheduling of the actuations. Additionally, the estimation and control gain calculations were broken up to limit the processing time of each task and care was taken to ensure their accuracy. The predictor-corrector formulation of the Kalman filter allows the time update of the estimate, or prediction, to be calculated separately from the measurement update, or correction. This application framework maintains consistent sampling and actuation times while addressing the limitations of the operating system.
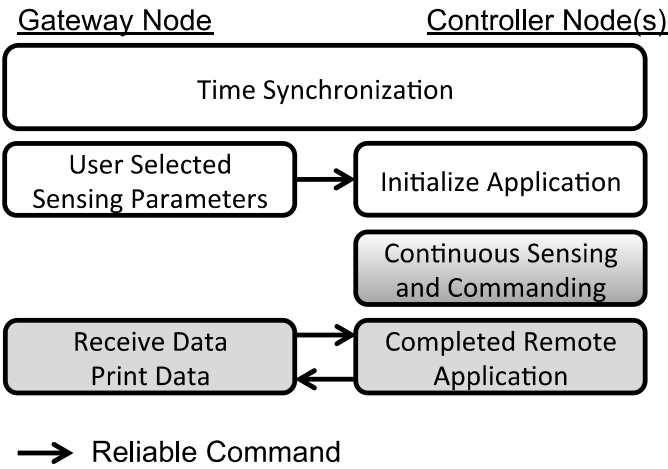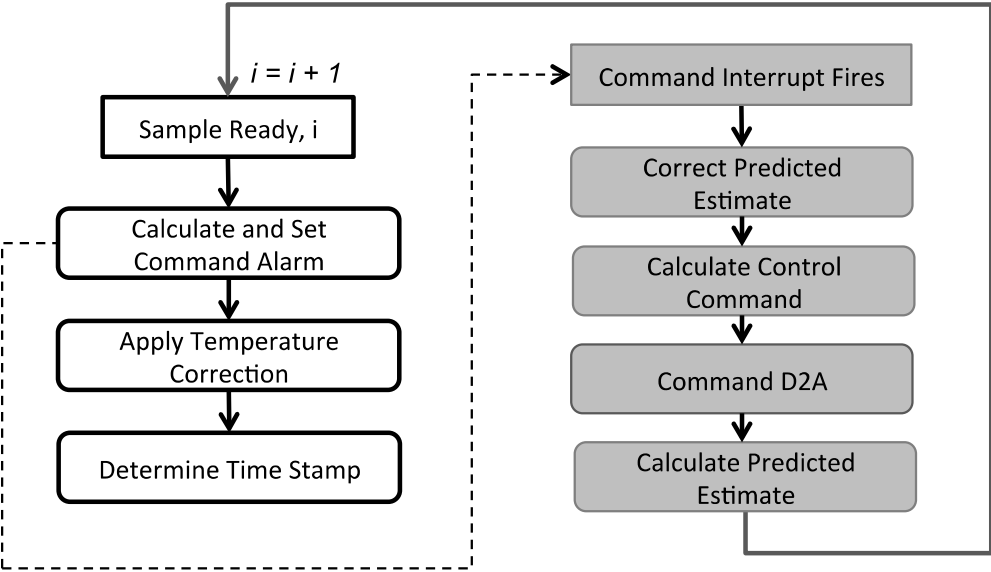
Fig. 4 Application Flowchart for Localized Control on WSN

Fig. 5 Sensing and Command Flowchart for Controller Node within Localized Control with an SHM-A

3. Experimental system

A single-story structure fitted with an active control system is used to evaluate the smart-sensor-based active control system, low-latency hardware, and discrete control design techniques. The active control system using the Imote2 smart sensor platform is compared to a wired system for performance evaluation.

3.1 System model

The experimental setup used for the active control experiment is shown in Fig. 6. The structure, manufactured by Quanser Consulting Inc., is a single-story building clamped to a fixed base. The aluminium columns have a section of 2 x 108 mm and an interstory height of 490 mm. The mass of the story is 1.662 kg and the mass of each column is 0.227 kg. The structure is fitted with an active mass driver (AMD) to control the structure. The mass of the AMD is 0.88 kg; although the mass of the AMD is a large percentage of the total structure, the goal of the experiment is to compare the performance of the two control systems. The AMD is fitted with a DC motor to move the cart along a geared track. An optical encoder is used to feedback the position of the cart along the 19 cm track. The position control of the cart is realized using a proportional derivative (PD) controller with encoder feedback. The control is implemented using a WinCon real-time controller on a PC fitted with a MultiQ I/O board. Finally, a capacitive DC accelerometer with a range of ±2g and a sensitivity of 1V/g was placed on the top story.

A system identification was conducted to develop a model of the experimental setup. A command displacement was issued to the AMD to excite the structure and the resulting AMD displacement and the acceleration of the top story were measured.
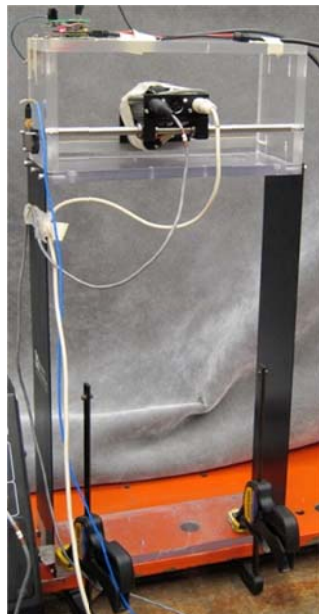

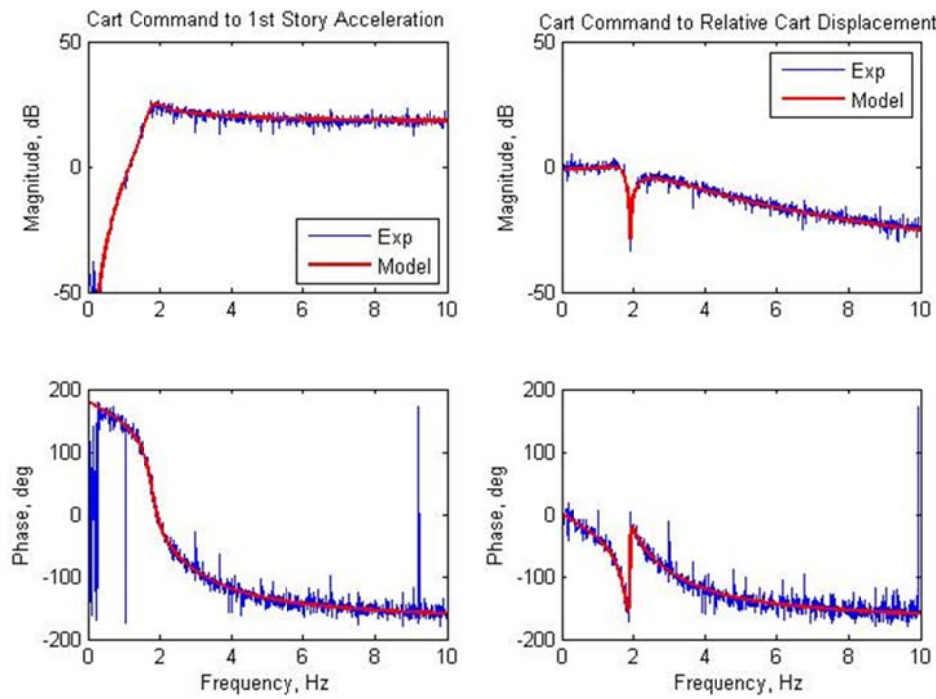Fig. 6 Single-Story Experimental Setup

Fig. 7 Experimental Transfer Function and Identified Model of Single-Story Setup

The resulting identified model is shown in Fig. 7; the experimental data is shown in blue and the identified model is shown in red. The identified model neglects the high-frequency dynamics of the motor, which results in a four-pole model. The high frequency dynamics of the motor would require a pole far into the left-half plane that is significantly faster than the system of interest; therefore, the pole can be neglected. The identified natural frequencies and damping are listed in Table 1. The first frequency corresponds to the structure and the second corresponds to the AMD. The identified damping in the first mode overestimates the damping in the structure, because experimentally the structure appears lightly damped. This overestimation is predominantly due to the mode of excitation. From the free-vibration response of the structure with no control and the 'locked' AMD, the experimentally determined damping is approximately 1.1% and 9.5%, respectively. The case with a 'locked' damper reflects the excitation used in the model development. The resulting identified model closely matches the experimental model in the frequency domain and can be used to in the control design to outperform the 'locked' damper case.

Table 1 Identified Natural Frequencies and Damping of Experimental Setup

Natural Frequency (Hz)	Damping (%)
1.81	11.9
2.59	58.3

3.2 Control design sampling rates

Three control systems are compared on the experimental setup: wired, Imote2+SHM-A, Imote2+SHM-SAR. Each system will operate at a different sampling rate based on the data acquisition approach and processing requirements. The wired system has no significant limitations on the possible sampling rate, so the wired control system will operate at 1000 Hz and can be approximated as continuous. As a result, this section will focus on the sampling rates for the two smart sensor systems.

As discussed in Section 2, the major difference between the two smart sensor systems is the data acquisition approach and the resulting sampling rate performance. The oversampling, pipeline style ADC on the SHM-A results in at least a 30 millisecond delay between a sample being taken and its availability on the processor (Linderman *et al*. 2015). On the other hand, the single-shot style ADC on the SHM-SAR limits the latency to about 200 microseconds (Linderman *et al*. 2015). This variation is sample availability on the processor impacts both the control software design on the Imote2 and the overall sampling rate of the control system. Ultimately, the sampling rate on the Imote2+SHM-A system is 25 Hz, which accounts for the 30-millisecond sampling delay, processing time, and any additional timing variations on the processor. On the other hand, the sampling latency on the SHM-SAR is almost negligible, so the sampling interval is entirely dependent on the processing time required; the resulting sampling rate for the Imote2+SHM-SAR is 950 Hz.

4. Discrete control design at slow sampling rates

An experimental control implementation typically requires a discrete-time representation of the controller. For systems with slow sampling rates or delays, a discrete-time control design can be essential. Because the Imote2+SHM-A smart sensor control system runs at a slow sampling rate, a discrete-time controller is necessary. Beyond ensuring the bandwidth of the system to be controlled is below the Nyquist frequency, the two important considerations for the performance of the discrete control design include: a discrete-time representation of the system and the inclusion of delays within the system model.

4.1 Discrete-time representation of the system to be controlled

Three common transformation techniques are used to develop discrete-time equivalents based on numerical integration (Franklin 1998); these techniques are illustrated in Fig. 8. The forward rectangular rule, or zero-order hold (ZOH), can create an unstable system because the resulting discrete-time poles do not necessarily lie within the unit circle. The backward rectangular rule forces the poles within the right-half plane of the unit circle. The trapezoid rule, commonly known as the Tustin method, always results in a stable system because the resulting poles must lie within the unit circle; however, this transformation can result in significant distortion. Another approach is an algorithm that tries to match the zero-pole equivalent in a discrete system and match the gain at the origin. All these approaches have advantages and disadvantages, but the two most common transformation approaches that will be addressed in this section is the ZOH and Tustin transformation.
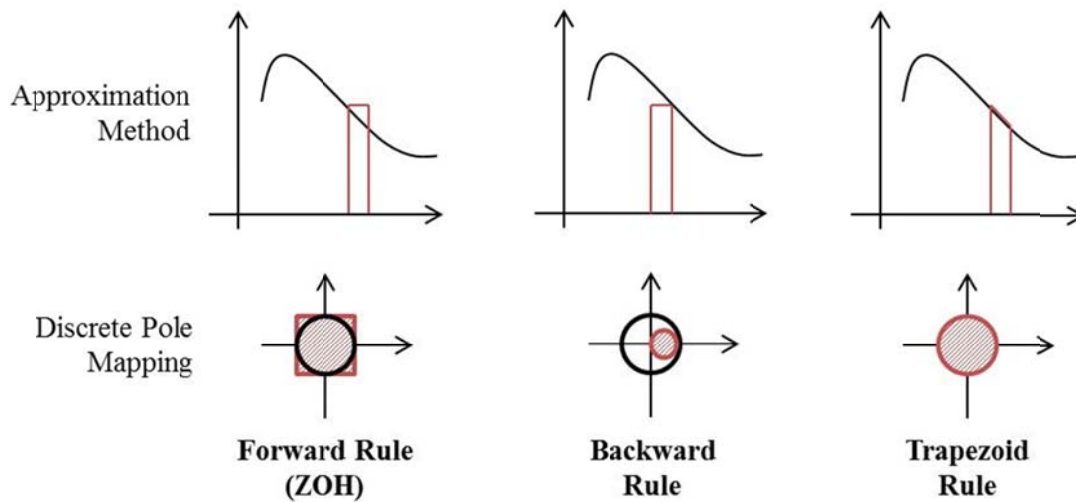
Fig. 8 Discrete Equivalent Transformation Techniques

One approach to control implementation is to transform a compensator designed in continuous time into discrete time. This transformation approach is common in wired control systems, because a fast sampling rate can be employed (Hirata and Powell 1990). Within wired control systems, the most common approach for transformation of the compensator designed in continuous into discrete time is the Tustin method, because it guarantees a stable system and can closely represent the controlled continuous-time system. However, when applied to systems with a slow sampling rate, transformed continuous-time controllers often result in instability and poorer performance. When using a ZOH transformation of the continuous controller, often an unstable control system results. Similarly, when a Tustin transform of the compensator is used, the discrete closed-loop system at the slow sampling rate is near the stability boundary. Therefore, a less authoritative compensator is required for stability in discrete-time. The instability and poorer performance using this control transform approach is due to the slow sampling rate and un-modeled internal delay present in a discretely sampled system.

For systems operating at a slow sampling rate, designing a controller directly on the discrete-equivalent of the system leads to a more consistently stable system and better control performance. An analytical model of a single-story system fitted with an AMD is used to compare the discrete time transformation of a system prior to control design. As shown in Fig. 9, the Tustin transformation gives much better results at approximating the continuous-time system in the frequency domain whereas the ZOH transformation gives poor results at the origin in both the magnitude and phase. However, a ZOH transformation ultimately results in a better control design because it approximates the sampled data system present in control.

A sample and hold system used in the control system can be directly modeled in discrete-time with a hold equivalent transform, as shown in Fig. 10. A sample and ZOH is an exact model for the sample and hold common in the A/D converter used in discrete control. Thus, a ZOH transform reflects the actual sampled system that will be encountered by the controller. In addition, a ZOH sampled system introduces a delay of T/2, where T is the sampling interval. This internal

delay is integrated into the model during the transform; and thus, the delay can be compensated for in the controller design. As a result, although the ZOH representation looks poorer in the frequency domain, a ZOH equivalent transform to a discrete-time model prior to control offers the best performance for a slowly sampled system.

4.2 Inclusions of delays within the system model

The time required for the sensing hardware, processing, and wireless communication results in at least a one-sample delay in the control system, which can be included as a sensor or input delay. The two different delay approaches are shown in Fig. 11, where the controller is represented by an estimator and control gain, K.
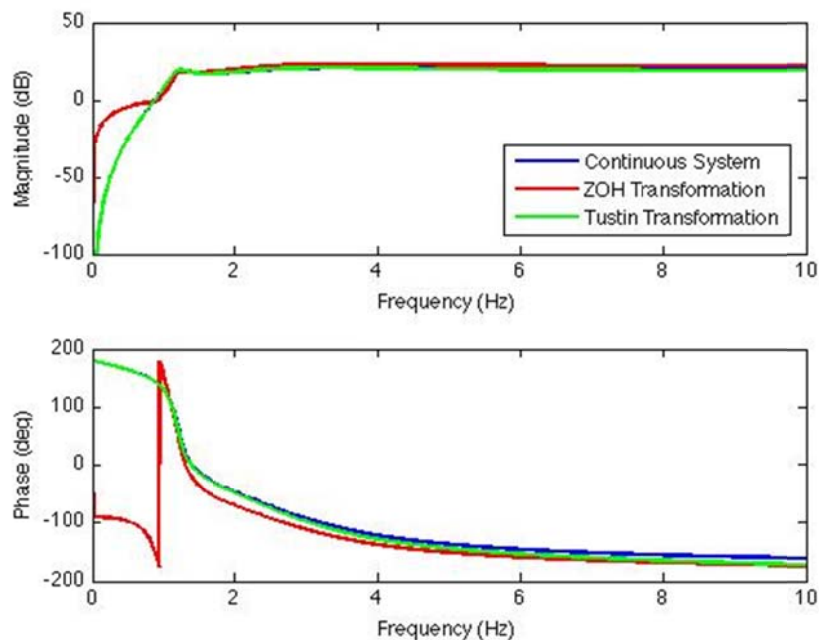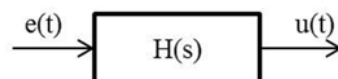

Fig. 9 Comparison of Discrete-Time Transformation Techniques in the Frequency Domain
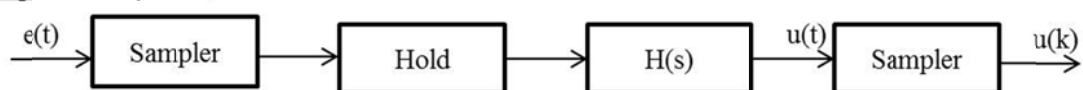

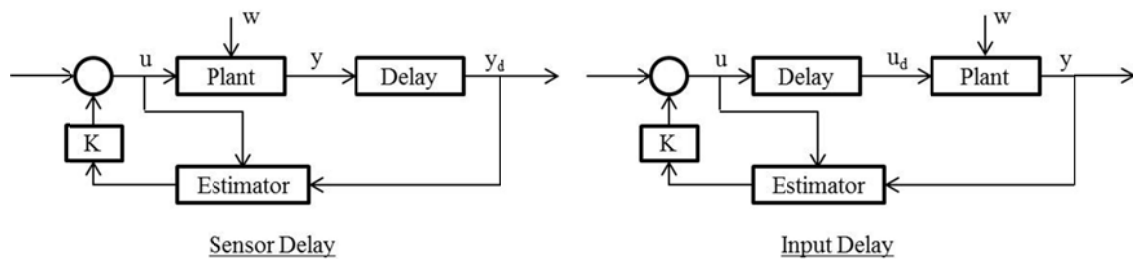Fig. 10 Equivalent Sample Hold System in Discrete-Time Control

Fig. 11 Delay Representations (Franklin 1998)

When a sensor delay is considered in the system, the system responds to a command input in exactly the same way as without the delay because the estimator sees the input command through the feedforward loop. However, the estimator is sensitive to disturbances through the delayed output (Franklin 1998). In addition, the delayed states are not weighted within the control gain, but are weighted within the estimator design. On the other hand, when an input delay is present in the system, the delays will be excited in the system response to an input command; and thus, the delayed system is used within the control design. However, the delayed states are not weighted within the estimator. In addition, the control feedback will be delayed before it can react to a disturbance to the plant, so the system is more sensitive to disturbances (Franklin 1998). As a result, the representation of the delay can impact the resulting control design and performance of the system.

In simulation, the two representations can result in comparable control performance if the delay is compensated for in the control design; however, the representation should adequately represent the delay present in the experimental system. Although the delay present in the wireless system appears to be a sensor delay, an input delay better reflects the experimental configuration because the controller computation occurs on the smart sensor platform prior to the application of control to the system. In addition, the estimator design based on an input delay requires slightly less computation because the delayed state is not weighted, which can be advantageous on a smart sensor platform. As a result, based on the experimental configuration, an input delay model should be used to include the delay present in wireless control systems.

Several approaches to modeling the input delay within the system model are available; however, not all approaches allow dynamic output feedback. Two common approaches that do allow dynamic output feedback include the Padé approximation in continuous systems and state augmentation in discrete systems (Sain *et al*. 1992, Franklin 1998). Because a continuous-time model is required for Padé delay states, an equivalent one step delay could be included in the continuous time system. However, the order of the Padé approximation is limited by the bandwidth of the system when converted to discrete-time. A Padé approximation was initially considered to incorporate a delay in the experimental model prior to discrete-time transformation, but the approach results in a system close to the stability boundary and poor closed-loop control performance under simulation in the presence of a time delay. Therefore, an input delay should be added to the discrete-time ZOH transformation of the system, described in the previous section, by including a delay state in the state-space representation:

$$\begin{bmatrix} x[k+1] \\ u_d[k+1] \end{bmatrix} = \begin{bmatrix} \Phi & \Gamma \\ 0 & 0 \end{bmatrix} \begin{bmatrix} x[k] \\ u_d[k] \end{bmatrix} + \begin{bmatrix} 0 \\ 1 \end{bmatrix} u(k) + \begin{bmatrix} \Gamma \\ 0 \end{bmatrix} w(k)$$

$$y(k) = \begin{bmatrix} 1 & 0 \end{bmatrix} \begin{bmatrix} x[k] \\ u_d[k] \end{bmatrix}$$

(1)

where u_d is the delayed input, Φ is the discrete-time state transition matrix, Γ is the discrete-time input matrix, x is the system state, and y is the measurement output at each step, k. Although the augmented state transition matrix is no longer full rank, the augmented system does satisfy the conditions for a solution to the linear quadratic regulator (LQR) control problem. This discrete-time state augmentation approach is the best solution for implementing an input delay within the system model and results in good compensation performance in simulation and experiments, as illustrated in section 6.

5. Control designs

5.1 Wired continuous control design

A wired control system is developed for comparison with the smart sensor implementation. Because the wired system operates at 1000 Hz, the wired system can be approximated as continuous. Therefore, this section presents the continuous control design that is implemented on the wired system.

Acceleration feedback has been shown to be effective in active structural control (Dyke *et al.* 1996, Spencer *et al.* 1998). Because acceleration measurements can be reliable and inexpensive, the system will use the story acceleration response as the primary measurement for control of the structure. Therefore, the control design will combine a Kalman estimator and linear quadratic regulator control design. A block diagram of the complete closed-loop system is given in Fig. 12. Furthermore, because the capacitive accelerometer provides a flat frequency response over the range of interest and zero phase lag, the sensor dynamics will be neglected in the design.

The LQR control design uses acceleration weighting to minimize the acceleration. To implement the acceleration weighting, the traditional LQR cost function is altered to

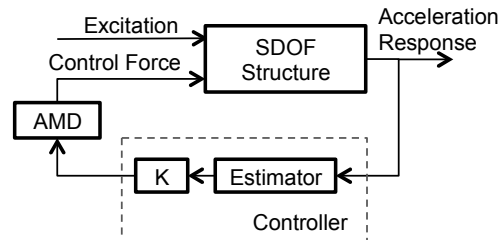$$J = \int_0^\infty \left[yQy + uRu \right] dt$$

(2)

Fig. 12 Block Diagram of the Active Feedback Control System

where *y* is the acceleration output, *Q* is the relative weighting on the measurement, *u* is the control effort, and *R* is the weighting on the control effort. For the control design in this case, the ratio of *Q/R* is varied and the root-mean-square (RMS) of the acceleration response and the control effort are determined based on numerical simulation. In simulation, the AMD is used to excite the structure prior to switching from excitation to control. The RMS of the acceleration normalized by the uncontrolled response is plotted versus the RMS of the control effort in Fig. 13. As the control force weighting, *R*, decreases, the additional control effort actually causes a worse response than the uncontrolled. The control design that resulted in a minimum response was selected; the selected controller design is highlighted with a red '*x*' in Fig. 13. The associated *Q* and *R* values are

$$Q = \begin{bmatrix} 1 \end{bmatrix} \quad R = \begin{bmatrix} 0.9955 \end{bmatrix}$$

An estimator is required to reconstruct the full-state response of the system based on the acceleration measurement. Because the process noise is hard to estimate within the system, the final estimator design is determined experimentally. A range of estimator designs is determined analytically and then applied experimentally with the same LQR control design. The estimator weightings that results in the best performance of the complete control system is selected as

$$S_w = \begin{bmatrix} 1 \end{bmatrix} \quad S_v = \begin{bmatrix} 10 \end{bmatrix}$$

5.2 Discrete control design for smart sensor implementation with the SHM-A

A discrete control design was developed for the Imote2 wireless smart sensor fitted with an SHM-A. As described in section 3.3, after combining the sensor latency with processing latency, a sampling interval of 40 milliseconds was selected, or a sampling rate of 25 Hz. Due to this slow sampling rate, a discrete control design is necessary. Following the design guidelines presented in section 4, a zero-order-hold discrete transformation of the system was determined that included an input delay through state augmentation.

Similar to the continuous control design, accelerometer weighting was used for the optimal discrete LQR control design. In numerical simulation, the AMD was again used to excite the structure prior to switching to control. The RMS acceleration normalized to the RMS uncontrolled response and RMS control effort is tabulated for a range of *Q/R* ratios. The normalized RMS acceleration response is plotted against the RMS control effort in Fig. 14. The control design selected minimizes the normalized RMS acceleration and is highlighted in Fig. 14 with a red '*x*'. The control design response weighting, *Q*, and control effort weighting, *R*, are

$$Q = \begin{bmatrix} 1 \end{bmatrix} \quad R = \begin{bmatrix} 2.6727 \end{bmatrix}$$

Therefore, the discrete control design results in a significantly different weighting design and subsequent control gain than the continuous system.

The accelerometer on the SHM-A was used for control feedback, due to its ease of implementation and the previous success with acceleration feedback in active structural control. A predictor-corrector formulation of the discrete-time Kalman filter was used for estimation. Similar to the continuous design, a range of estimators determined analytically were experimentally implemented to determine the best estimator given the process and sensor noise in the system. The estimator that resulted in the best overall control performance was selected. The resulting process

and sensor noise weightings are

$$S_w = [1] \quad S_v = [100]$$

The larger noise weighting is due to the higher noise floor of the accelerometer on the SHM-A in addition to the noise added through aliasing during decimation. As expected, the resulting discrete-time design differs from the continuous control design.
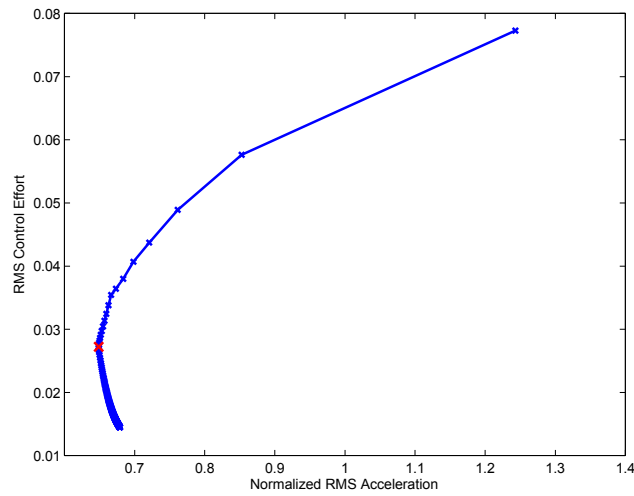

Fig. 13 Summary of Continuous LQR Control Designs with Selected Design Highlighted
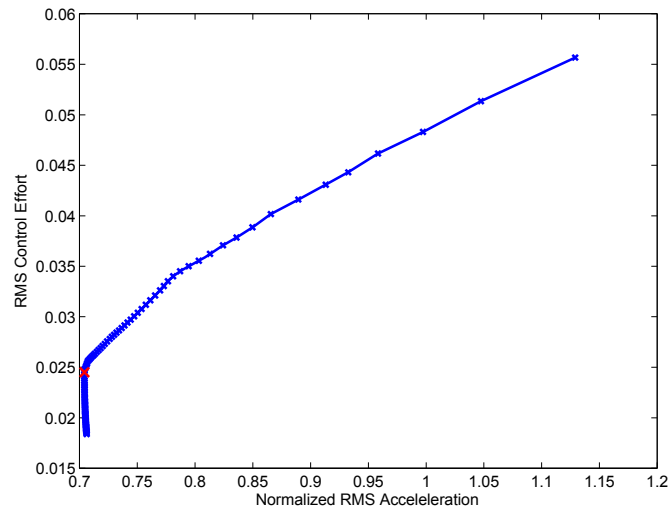

Fig. 14 Summary of Discrete LQR Control Designs for SHM-A with Selected Design Highlighted

5.3 Discrete control design for smart sensor implementation with SHM-SAR

In addition, a discrete control design was developed for the Imote2 wireless smart sensor fitted with an SHM-SAR data acquisition board. Given the limited latency in data acquisition, a sampling rate of 950 Hz was selected. Although this sampling rate is comparable to the wired system, a discrete control design approach was used because it will ultimately be implemented on the smart sensor platform. The control application uses the discrete-time predictor-corrector formulation of the Kalman Filter. In addition, an input delay was included in the design to account for the one sample delay in the control application. Following the design guidelines presented in section 4, a zero-order-hold discrete transformation of the system that included an input delay through state augmentation was used for design.

Similar to the previous discrete control design, the normalized RMS acceleration response and the corresponding RMS control effort was determined. The control design that minimized the normalized RMS acceleration response was selected. The control design response weighting, Q, and control effort weighting, R, are

$$Q = \begin{bmatrix} 1 \end{bmatrix} \quad R = \begin{bmatrix} 1.1697 \end{bmatrix}$$

As the sampling rate increases, the control design will approximate the continuous control design with an input delay.

A wired accelerometer was used for control feedback in conjunction with the SHM-SAR, due to its ease of implementation, previous success, and for comparison with the other control systems. A predictor-corrector formulation of the Kalman filter was used for estimation on the Imote2. Similar to the previous designs, the estimator that resulted in the best overall control performance was selected. The resulting process and sensor noise weightings are

$$S_w = \begin{bmatrix} 1 \end{bmatrix} \quad S_v = \begin{bmatrix} 10 \end{bmatrix}$$

The noise weighting is the same as the wired design, because the same accelerometer is used and little additional noise is added due to the SAR-based data acquisition. However, the resulting estimator gain matrix is different due to the discrete-time time design, as expected.

6. Experimental results

The previous control designs have been implemented on the single-story experimental structure to validate the use of the smart sensor platform for active structural control. Five different configurations were considered for the validation: uncontrolled, zeroed control, wired control, smart sensor control with the SHM-A, and smart sensor control with the SHM-SAR. For the uncontrolled configuration, the AMD was fixed to the side of the structure; therefore, the additional mass due to the cart was still present but otherwise did not influence the response. In zeroed control, a zero displacement command was issued to the AMD. Schematics of the wired and smart sensor control experimental setups are provided in Figs. 15(a)-15(c), respectively. In the schematics, the solid red lines represent analog signals and the dashed red line represents the digital encoder signal. The blue lines represent the computer control calculations and the green lines represent the smart sensor node.

(a) Wired Experimental Setup   (b) Smart Sensor Experimental Setup, SHM-A

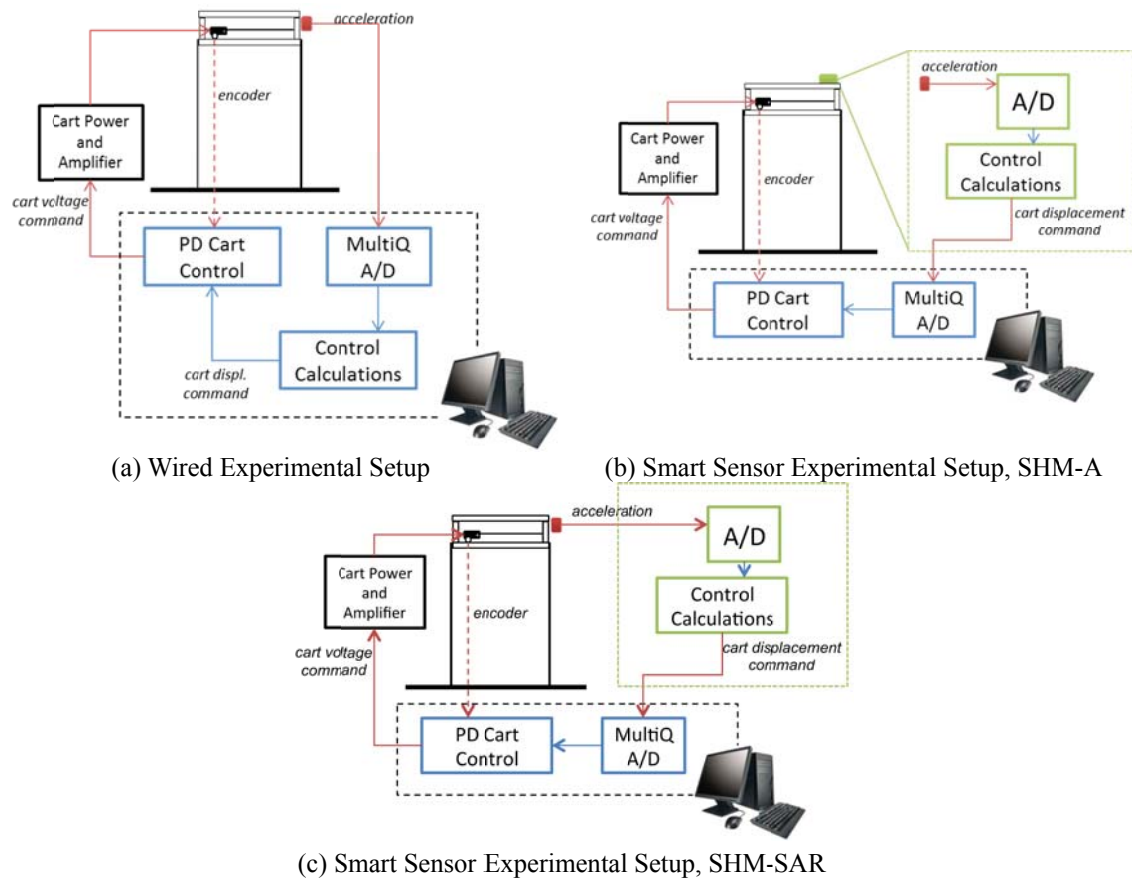(c) Smart Sensor Experimental Setup, SHM-SAR

Fig. 15 Schematics of Wired and Smart Sensor Control Experimental Setups

In the wired system (Fig. 15(a)), the acceleration feedback is passed to the control computer through the MultiQ A/D. The continuous control design programmed onto the computer calculates the required cart displacement command. The displacement command is converted to an appropriate voltage through the PD cart control, which uses the encoder feedback. The voltage is then applied to the AMD through the amplifier and power source.

On the other hand, in the smart sensor system (Fig. 15(b)), the smart sensor node is responsible for the acceleration measurement and control calculations. The control implementation on the Imote2 platform is programmed with the discrete control design discussed previously. The resulting cart displacement command is issued as an analog voltage from the SHM-D2A to the MultiQ board for the PD control of the AMD. The control computer then outputs the required voltage to the AMD, which is applied through the cart amplifier. The control computer is used for the PD control of the AMD rather than the wireless smart sensor because the SHM-A cannot currently handle the encoder feedback required for displacement control.

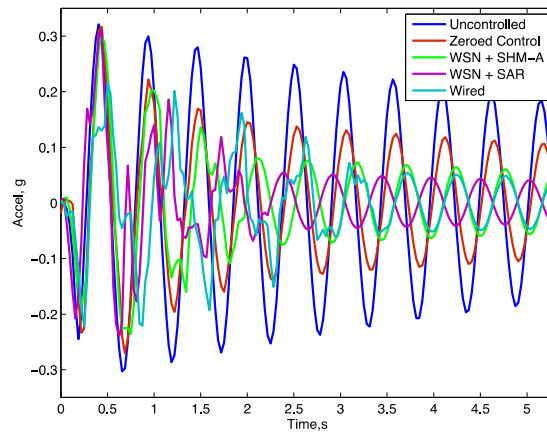Two other considerations in the smart sensor experimental control implementation include the
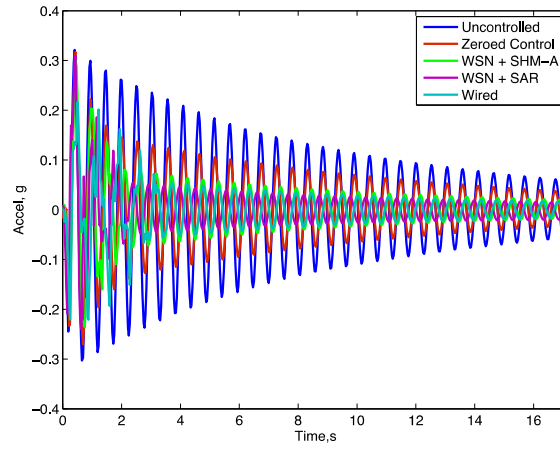
accelerometer calibration and the resolution of the MultiQ A/D. The offset and scale factors of the *x*-axis on the SHM-A accelerometer were determined using static calibration (Jang and Rice 2009). Because the model was not originally identified using the SHM-A, the accelerometer measurements must be scaled appropriately for successful control implementation. The second consideration is the resolution of the MultiQ A/D. Because the required AMD displacements are small values when scaled in meters, the full voltage range of the MultiQ A/D input is not used; therefore, the 12-bit resolution of the MultiQ ADC is an issue. The output was multiplied by 10 on the Imote2 prior to conversion to obtain better resolution of the command input and stay within the output range of the SHM-D2A.

Similarly, for the smart sensor experimental implementation with the SHM-SAR (Fig. 15(c)), the wired accelerometer output, span of the SHM-SAR A/D, and the resolution of the MultiQ A/D need to be considered. In this case, a wired accelerometer is used and output has to be appropriately shifted and scaled for use with the data acquisition board. The capacitive accelerometer offers the ability to shift the DC offset to 1.25 V, or the mean of the input voltage range. The mean value is then removed in software on the Imote2 prior to control calculations. The control output is again multiplied by 10 on the Imote2 prior to conversion to obtain better resolution of the command input on the MultiQ A/D and stay within the output range of the SHM-D2A.
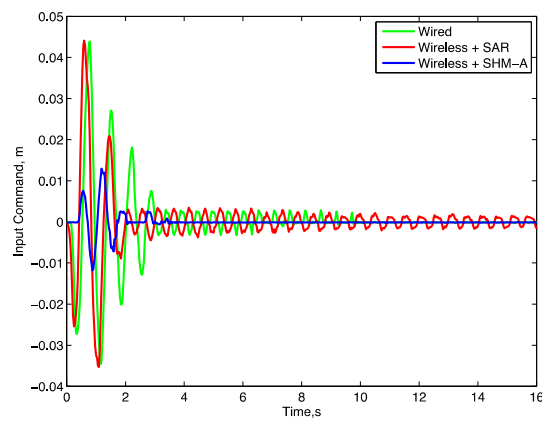
In the experiment, an initial displacement was applied to the structure and then released to obtain the free response of the structure for each control configuration. A comparison of the responses for the five configurations is provided in Fig. 16 and the normalized RMS acceleration response is given in Table 2. The uncontrolled response, shown in blue, reflects the general damped free response of a structure. The zeroed response, shown in red, has a significantly faster decay in the response than the uncontrolled. Therefore, the AMD with a zero command introduces significant damping to the system due to the friction and slight motion of the AMD. The wired system, shown in cyan, achieves a significant reduction in the response. The smart sensor system with the SHM-A, shown in green, achieves comparable performance to the wired system; however, the performance is not as good initially. This result is likely due to the slow sampling rate. The smart sensor system with the SHM-SAR, shown in pink, performs as well as the wired system. Thus, the discrete-time control implementation on the smart sensor was able to achieve a similar reduction in the response as the continuous-time wired controller. Additionally, the new data acquisition hardware developed for wireless structural control (SHM-SAR) outperforms the SHM-A.

In both controlled cases, the control predominantly occurs during the beginning of the response. As shown in Fig. 16(b), the control effort alters both the magnitude and frequency of the response for both the wired and smart sensor systems. The responses during the initial period lie within the zeroed control response and then are reduced further. At about three seconds, the control efforts are within the friction of the device and the systems return to free response. The smart sensor control efforts are significantly lower than the wired system and still achieve comparable performance (Fig. 16(c)).

Overall, the experimental results highlight the successful implementation of active structural control using a wireless smart sensor platform. By properly accounting for discrete-time control design at slow sampling rates, the smart sensor implementation achieves comparable performance to the wired system and no instability occurred.

(b)

(c)

Fig. 16 (a) Comparison of Experimental Response of Small-Scale Setup (b) Zoom Over the Region of Control (c) Corresponding Control Command

Table 2 Normalized RMS Acceleration Responses for Single-story Experimental Setup

Experimental Configuration	RMS Acceleration Response Normalized to Uncontrolled
Zeroed Control	0.642
Smart Sensor Control - SHM-A	0.482
Smart Sensor Control - SHM-SAR	0.398
Wired Control	0.399

7. Conclusions

This work addresses control design at slow sampling rates, compensation for time delays, and the significance of data acquisition hardware in achieving smart sensor based active control. Because active control systems do not guarantee stability, their application requires attention to all the elements of the control loop, including the design at slow sampling rates, data acquisition hardware, and processing performance, which are typically neglected. These elements of an active control loop are presented in the context of a single-story structure fitted with an active mass damper. Two different types of digital-to-analog converters are considered to highlight the significance of data acquisition and hardware in using wireless sensor networks for control. The resulting slow sampling rate of smart sensor nodes requires careful consideration of the system model and delay representation used for design. The two smart sensor control systems offer good experimental control performance. In addition, the lower-latency data acquisition approach achieves equal performance to the wired system used as a baseline, underscoring the importance of thoughtful control design and hardware selection.

Acknowledgments

References

Casciati, S. and Chen, Z.C. (2012), "An active mass damper system for structural control using real-time wireless sensors", *Struct. Control Health Monit.*, **19**(8), 758-767. DOI: 10.1002/stc:1485.

Chu, S.Y., Soong, T.T., Lin, C.C. and Chen, Y.Z. (2002), "Time-delay effect and compensation on direct output feedback controlled mass damper systems", *Earthq. Eng. Struct. D.*, **31**, 121-137. DOI: 10.1002/eqe.101

Chung, L.L., Lin, C.C. and Lu, K.H. (1995), "Time-delay control of structures", *Earthq. Eng. Struct. D.*, **24**(5), 687-701. doi:10.1002/eqe.4290240506

Dyke, S.J., Spencer Jr, B.F., Quast, P., Kaspari Jr, D.C. and Sain, M.K. (1996), "Implementation of an active mass driver using acceleration feedback control", *Microcomput. Civil Eng.*, **11**, 305-323.

Franklin, G., Powell, J. and Workman, M. (1998), *Digital Control of Dynamic Systems*, 3rd Ed., California: Ellis-Kagle Press.

Hirata, H. and Powell, J.D. (1990), "Sample rate effects on disturbance rejection for digital control systems",

Proceedings of the American Controls Conference, San Diego, CA.

Housner, G.W., Bergman, L.A., Caughey, T.K., Chassiakos, A.G., Claus, R.O., Masri, S.F., Skelton, R.E., Soong, T.T., Spencer, B.F. and Yao, J.T.P. (1997), "Structural control: past, present, and future", *J. Eng. Mech. - ASCE*, **123**(9), 897-972. doi:10.1061/(ASCE)0733-9399(1997)123:9(897).

Jang, S. and Rice, J. (2009), "Calibration guide for wireless smart sensors. Illinois structural health monitoring project", http://shm.cs.uiuc.edu/files/docs/CalibrationGuide.pdf (last accessed April 16, 2012).

Jo, H., Sim, SH., Mechitov, K.A., Kim, R., Li, J., Moinzadeh, P., Spencer Jr., B.F., Park, J.W., Cho, S., Jung, H.J., Yun, C.B., Rice, J.A. and Nagayama, T. (2011), "Hybrid wireless smart sensor network for full-scale structural health monitoring of a cable-stayed bridge", *Proceedings of SPIE Conference*, San Diego, CA.

Levis, P., Madden, S., Polastre, J., Szewczyk, R., Woo, A., Gay, D., Hill, J., Welsh, M., Brewer, E. and Culler, D. (2005), "TinyOS : An Operating System for Sensor Networks", Ambient Intelligence, ed. Werner Weber, Jan M. Rabaey, and Emile Aarts, 115-147. Springer, Berlin, Heidelberg.Tavel, P. 2007 Modeling and Simulation Design. AK Peters Ltd.

Linderman, L.E. (2013), *Smart Wireless Control of Civil Structures*, Ph.D. Dissertation, Department of Civil and Environmental Engineering, University of Illinois at Urbana-Champaign, Illinois.

Linderman, L.E., Mechitov, K. and Spencer, B.F. (2013), "TinyOS-based real-time wireless data acquisition framework for structural health monitoring and control", *Struct. Control Health Monit.*, **20**(6), 1007-1020. DOI: 10.1002/stc.1514.

Linderman, L.E., Jo, H. and Spencer, B.F. (2015), "Low-latency data acquisition hardware for real-time wireless sensor applications", *IEEE Sens. J.*, **15**(3), 1800-1809. DOI: 10.1109/JSEN.2014.2366932

Loh, C.H., Lynch, J.P., Lu, K.C., Wang, Y., Chang, C.M., Lin, P.Y. and Yeh, T.H. (2007), "Experimental verification of a wireless sensing and control system for structural control using MR dampers", *Earthq. Eng. Struct. D.*, **36**(3), 1303-1328.

Lynch, J.P. and Loh, K. (2006), "A summary review of wireless sensors and sensor networks for structural health monitoring", *Shock Vib.*, **38**(2), 91-128.

Lynch, J.P., Wang, Y., Swartz, R.A., Lu, K.C. and Loh, C.H. (2008), "Implementation of a closed-loop structural control system using wireless sensor networks", *Struct. Control Health Monit.*, **15**(4), 518-539.

Rice, J.A. and Spencer Jr., B.F. (2009), *Flexible Smart Sensor Framework for Autonomous Full-scale Structural Health Monitoring*, Newmark Structural Engineering Laboratory Report Series, Vol. 18, University of Illinois at Urbana-Champaign, Illinois. http://hdl.handle.net/2142/13635.

Rice, J.A., Mechitov, K.A., Sim, S.H., Spencer Jr., B.F. and Agha, G.A. (2011), "Enabling framework for structural health monitoring using smart sensors", *Struct. Control Health Monit.*, **18**(5), 574-587. DOI:10.1002/stc.386.

Sain, P.M., Spencer Jr, B.F., Sain, M.K. and Suhardjo, J. (1992), "Structural control design in the presence of time delays", *Proceedings of the ASCE Engineering Mechanics Conference*, College Station, Texas.

Soong, T.T. (1990), *Active Structural Control: Theory and Practice*, Essex, England: Longman Scientific & Technical.

Spencer, B.F., Dyke, S.J. and Deoskar, H.S. (1998), "Benchmark problems in structural control: part I—Active Mass Driver system", *Earthq. Eng. Struct. D.*, **27**(11), 1127-1139.

Swartz, A., Jung, D., Lynch, J.P., Wang, Y., Shi, D. and Flynn, M.P. (2005), "Design of a wireless sensor for scalable distributed in-network computation in a structural health monitoring system", *Proceedings of the 5th International Workshop on Structural Health Monitoring*, Stanford, CA.

Wang, Y., Swartz, R.A., Lynch, J.P., Law, K.H., Lu, K.C. and Loh, C.H. (2006), "Decentralized civil structural control using a real-time wireless sensing and control system", *Proceedings of the 4th World Conference on Structural Control and Monitoring*, San Diego, CA.

Wang, Y., Swartz, R.A., Lynch, J.P., Law, K.H., Lu, K.C. and Loh, C.H. (2007), "Decentralized civil structural control using real-time wireless sensing and embedded computing", *Smart Struct. Syst.*, **3**(3), 321-340.

CY